The Effect of Charged Axial Ligands on the EPR Parameters in Oxovanadium(IV) Compounds: An Unusual Reduction of the $A_z(^{51}V)$ Values

Evangelos J. Tolis,[a] Vasilios I. Teberekidis,[b] Catherine P. Raptopoulou,[c] Aris Terzis,[c] Michael P. Sigalas,[b] Yiannis Deligiannakis,*[d] and Themistoklis A. Kabanos*[a]

Abstract: Two series of octahedral oxovanadium(IV) compounds, containing charged or neutral axial ligands, with the tetradentate amidate molecules Hcapca and H_2capcah of the general formulae *trans*-$[V^{IV}OX(capca)]^{0/+}$ (where $X = Cl^-$ (**1**·CH_2Cl_2), SCN^- (**2**), N_3^- (**3**), CH_3COO^- (**4**), $PhCOO^-$ (**5**), imidazole (**6**·CH_3NO_2), and η-*n*$BuNH_2$ (**7**)) and *cis*-$[V^{IV}OX(Hcapcah)]^{0/+}$ (where $X = Cl^-$ (**8**·$0.5\,CH_2Cl_2$), SCN^- (**9**), N_3^- (**10**·$2\,CH_3OH$), and imidazole (**11**)), were synthesized and characterized by X-ray crystallography (**1**·CH_3OH, **8**·$CHCl_3$, **9**·$2\,CH_3CN$, **10**·CH_3CN and *cis*-$[VO(imidazole)(Hcapcah)]^+$) and continuous-wave electron paramagnetic resonance (cw EPR) spectroscopy. In addition to the synthesis, crystallographic and EPR studies, the optical, infrared and magnetic properties (room temperature) of these compounds are reported. Ab initio calculations were also carried out on compound **8**·$CHCl_3$ and revealed that this isomer is more stable than the *trans* isomer, in good agreement with the experimental data. The cw EPR studies of compounds **1**–**5**, that is, the $V^{IV}O^{2+}$ species containing *monoanionic* axial ligands, revealed a novel phenomenon of the reduction of their A_z components by about 10% relative to the N_4 reference compounds ($[V^{IV}O(imidazole)_4]^{2+}$ and $[V^{IV}O(2,2\text{-bipyridine})_2]^{2+}$, see reference [46]). In marked contrast, such a reduction is not observed in compounds **6**·CH_3NO_2–**11**, which contain *neutral* axial ligands. Based on the spin-Hamiltonian formalism a theoretical explanation is put forward according to which the observed reduction of A_z is due to a reduction of the electron–nuclear dipolar coupling (P). The present findings bear strong relevance to cw EPR studies of oxovanadium(IV) in vanadoproteins, $V^{IV}O^{2+}$-substituted proteins, and in $V^{IV}O^{2+}$ model compounds, since the hyperfine coupling constant, A_z, has been extensively used as a benchmark for identification of equatorial-donor-atom sets in oxovanadium(IV) complexes.

Keywords: ab initio calculations · coordination modes · EPR spectroscopy · imidazole · vanadium

Introduction

Vanadium is a bioessential element that is found in remarkably high concentrations in marine ascidians,[1] in certain mushrooms,[2] and in polychaete worms.[3] In addition, two classes of vanadium enzymes, vanadium nitrogenases[4] and vanadate-dependent haloperoxidases,[5] found in nature, as well as the vanadium's insulinomimetic action[6] have spurred a considerable amount of research by bioinorganic[7] and coordination chemists,[7] biochemists etc. In addition, the oxovanadium(IV) cation ($V^{IV}O^{2+}$) has been used in electron paramagnetic resonance (EPR), electron spin-echo envelope modulation (ESEEM), and electron nuclear double resonance (ENDOR) studies as a spin probe[8–24] of naturally occurring vanadoproteins, in proteins in which the EPR silent divalent cations (Mg^{2+}, Ca^{2+}, etc.) have been substituted by $V^{IV}O^{2+}$, and in model $V^{IV}O^{2+}$ compounds.

Oxovanadium(IV) compounds are typically five- or six-coordinate, with the V=O bond practically defining the axial direction (z) of the local geometry. This gives rise to an approximate axial $^{51}V(I = 7/2)$ hyperfine matrix (A) with strong anisotropy, that is, usually $A_x \sim A_y \ll A_z$.[8] Differences in the four equatorial ligands give rise to differences in the $^{51}V(I = 7/2)$ hyperfine couplings, mainly in the principal A_z value. In general, the effect of the equatorial ligands on the $A(^{51}V)$ and $g(^{51}V)$ values can be explained by the model of

[a] Dr. T. A. Kabanos, E. J. Tolis
Department of Chemistry
Section of Inorganic and Analytical Chemistry
University of Ioannina, 451 10 Ioannina (Greece)
E-mail: tkampano@cc.uoi.gr

[b] V. I. Teberekidis, Dr. M. P. Sigalas
Department of Chemistry
Laboratory of Applied Quantum Chemistry
Aristotle University of Thessaloniki
540 06 Thessaloniki (Greece)

[c] Dr. C. P. Raptopoulou, Prof. Dr. A. Terzis
NRCPS Demokritos, Institute of Materials Science
15 310 Agia Paraskevi Attikis (Greece)

[d] Dr. Y. Deligiannakis
Department of Environmental and Natural Resources
Laboratory of Physical Chemistry
University of Ioannina, Pyllinis 9, 30100 Agrinio (Greece)
E-mail: ideligia@cc.uoi.gr

  0947-6539/01/0712-2698 $ 17.50+.50/0

Ballhausen and Gray.[25] In oxovanadium(IV) compounds with symmetries that do not deviate significantly from C_{4v}, the unpaired electron resides mainly on the nonbonding d_{xy} orbital and thus, the spin-hamiltonian parameters A_x, A_y, A_z and g_x, g_y, g_z are mainly affected by the bonding properties of the equatorial ligands, while an axial ligand *trans* to the oxo moiety has usually no resolvable effect on these parameters. Therefore, the weakly associated axial ligands are ignored in the analysis of the $A(^{51}V)$ and g values. In this context, a correlation is predicted to exist between the A_z and g_z values as a function of the bonding properties of the equatorial ligands. Experimentally, this correlation between g_z versus A_z is well documented for various oxovanadium(IV) compounds,[8] even for cases where the local symmetry deviates from C_{4v}.[26, 27] As a result, in a $g_z(^{51}V)$ versus $A_z(^{51}V)$ plot the data lie approximately on a straight line with negative slope.[26] Physically, this correlation between g_z versus A_z can be interpreted within the Ballhausen-Gray[25] model by assuming that increased in-plane π and σ bonding results in decreased A_z (^{51}V) and increased g_z (^{51}V) values (for a recent discussion see reference [26]). Inherent in this interpretation of the g_z versus A_z correlation is the assumption that other pertinent physical parameters, that is, the Fermi contact term (K) and the electron–nuclear dipole interaction (P) are invariant. The correlation between A_z and g_z has been used to identify the $V^{IV}O^{2+}$ ion's coordination sphere in a number of oxovanadium(IV) compounds.[11, 26–28] Substantial deviations from the aforementioned linear g_z versus A_z correlation imply that the physical picture and/or the approximations made should be reassessed.

Recently, we have reported that a substantial deviation from the locus of $g_z - A_z$ correlation plot is observed in certain oxovanadium(IV) compounds that contain axial anionic ligands,[29] for example, Cl^-. To the best of our knowledge, there are only two other structurally characterized $V^{IV}O^{2+}$ species with a monoanionic ligand (Cl^-) in axial position.[30] This is mainly due to the facts that i) the total ligand charge in the equatorial plane is at least -2[31] or even higher[32] and ii) a monoanionic ligand prefers an equatorial ligation.[33] Therefore we designed a tetradentate amidate ligand, hereafter abbreviated as Hcapca, with conjugated double bonds,

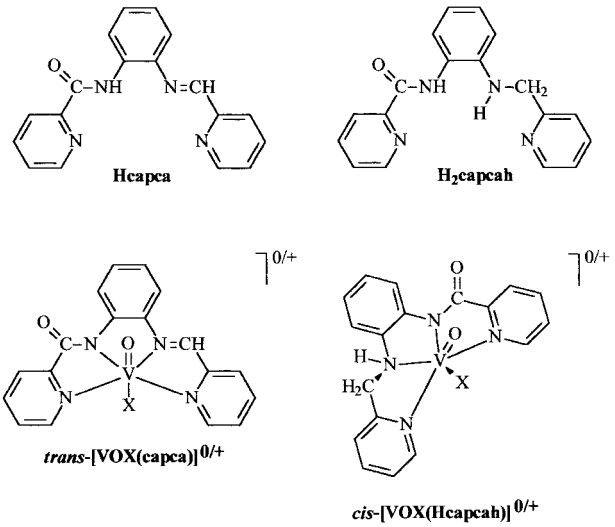

imposing planar or quasi-planar conformation and maximum equatorial negative charge of -1 upon coordination to vanadium. Reduction of the Hcapca at −C=N− double bond breaks the conjugation of Hcapca and results in the formation of a more flexible ligand abbreviated as H_2capcah. Herein, we wish to report the synthesis, structural, and cw EPR characterization of two series of oxovanadium(IV) compounds of the general formulae *trans*-$[V^{IV}OX(capca)]^{0/+}$ and *cis*-$[V^{IV}OX(Hcapcah)]^{0/+}$ (X = either a monoanionic ligand e.g., Cl^-, SCN^-, N_3^- etc. or a neutral ligand e.g., imidazole) with the view to studying the effect of the charged axial ligands on the ^{51}V hyperfine coupling constants and in particular on the parallel component, A_z. In addition, the optical and infrared spectra of the oxovanadium(IV) compounds are reported as well as a theoretical analysis of the geometry of the *cis*-[VOCl(Hcapcah)] based on density functional theory (DFT).

Abstract in Greek: Δύο σειρές οκταεδρικών ενώσεων του οξοβαναδίου(IV), που περιέχουν φορτισμένους ή ουδέτερους αξονικούς υποκαταστάτες, με τα τετραδοντικά αμιδικά μόρια Hcapca και H_2capcah των γενικών τύπων *trans*-$[V^{IV}OX(capca)]^{o/+}$ [όπου X=Cl^- (**1**•CH_2Cl_2), SCN^- (**2**), N_3^- (**3**), CH_3COO^- (**4**), $PhCOO^-$ (**5**), ιμιδαζόλιο (**6**•CH_3NO_2) και *η*-$BuNH_2$ (**7**)] και *cis*-$[V^{IV}OX(Hcapcah)]^{o/+}$ [όπου X=Cl^- (**8**•0.5CH_2Cl_2), SCN^- (**9**), N_3^- (**10**•2CH_3OH) και ιμιδαζόλιο (**11**)], συντέθηκαν και χαρακτηρίστηκαν κρυσταλλογραφικά {**1**•CH_3OH, **8**•$CHCl_3$, **9**•2CH_3CN, **10**•CH_3CN και *cis*-$[V^{IV}O$(ιμιδαζόλιο)(Hcapcah)$]^+$} και με φάσματα ηλεκτρονικού παραμαγνητικού συντονισμού (EPR). Τα φάσματα ορατού και υπερύθρου, καθώς και οι μαγνητικές ιδιότητες (θερμοκρασία περιβάλλοντος) των ενώσεων του οξοβαναδίου(IV) μελετήθηκαν επίσης. Θεωρητικοί υπολογισμοί *ab initio* έγιναν για την ένωση *cis*-$[V^{IV}OCl$(Hcapcah)$]$•$CHCl_3$ (**8**•$CHCl_3$) και έδειξαν ότι αυτό το ισομερές είναι πιο σταθερό από το *trans*-ισομερές, σε συμφωνία με τα πειραματικά δεδομένα. Οι μελέτες EPR των ενώσεων **1**•CH_2Cl_2 - **5**, δηλαδή των ενώσεων του $V^{IV}O^{2+}$ που περιέχουν μονοανιονικούς αξονικούς υποκαταστάτες, φανέρωσαν ένα καινούργιο φαινόμενο της μείωσης των A_z παραμέτρων κατά περίπου 10% σε σύγκριση με τις N_4 ενώσεις αναφοράς {$[V^{IV}O$(ιμιδαζόλιο)$_4]^{2+}$ και $[V^{IV}O$(2,2-διπυριδίνη)$_2]^{2+}$}. Σε σαφή αντίθεση, τέτοια μείωση δεν παρατηρείται στις ενώσεις **6**•CH_3NO_2 - **11**, που περιέχουν ουδέτερους αξονικούς υποκαταστάτες. Βασισμένοι στο φορμαλισμό της Χαμιλτονιανής του σπιν προτείνεται μια θεωρητική εξήγηση, σύμφωνα με την οποία η παρατηρούμενη μείωση των τιμών A_z οφείλεται στη μείωση της διπολικής αλληλεπίδρασης ηλεκτρονίου-πυρήνα (P). Τα αποτελέσματα της μελέτης αυτής έχουν μεγάλη σχέση με τις μελέτες EPR του οξοβαναδίου(IV) στις βαναδοπρωτεΐνες, και στις $V^{IV}O^{2+}$ - υποκατεστημένες πρωτεΐνες και στις $V^{IV}O^{2+}$ - πρότυπες ενώσεις, αφού η τιμή A_z χρησιμοποιείται εκτεταμένα ως παράμετρος αναφοράς για την ταυτοποίηση των ατόμων δοτών στο ισημερινό επίπεδο στις ενώσεις του οξοβαναδίου(IV).

Results and Discussion

Synthesis of the compounds: The reduced analogue of Hcapca, that is H_2capcah, was prepared by using a Pd catalyst (10% Pd on activated carbon) and pure hydrogen as reducing agent. The synthesis of the oxovanadium(IV) compounds with the ligands Hcapca and H_2capcah is summarized in Scheme 1.

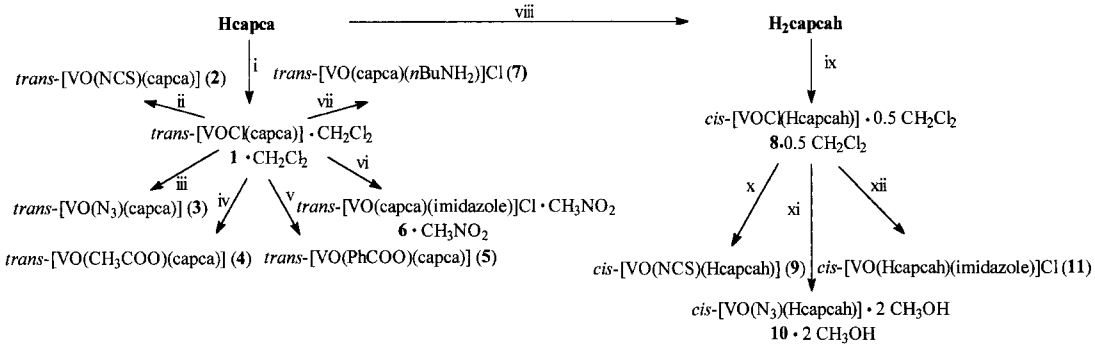

Scheme 1. Synthesis of the oxovanadium(IV) compounds with Hcapca and its reduced analogue H_2capcah. Conditions: i) $[VOCl_2(thf)_2]$, Et_3N, CH_3OH; ii) **1**·CH_2Cl_2, Et_4NSCN, CH_3OH; iii) **1**·CH_2Cl_2, Et_4NN_3, CH_3OH; iv) **1**·CH_2Cl_2, CH_3COOH, Et_3N, CH_3CN; v) **1**·CH_2Cl_2, PhCOOH, Et_3N, CH_3CN; vi) **1**·CH_2Cl_2, imidazole, CH_3NO_2; vii) **1**·CH_2Cl_2, η-nBuNH$_2$, CH_2Cl_2; viii) Hcapca, 10% Pd on activated carbon, H_2, CH_3OH; ix) $[VOCl_2(thf)_2]$, Et_3N, CH_3OH; x) **8**·0.5CH_2Cl_2, Et_4NSCN, CH_3OH; xi) **8**·0.5CH_2Cl_2, Et_4NN_3, CH_3OH; xii) **8**·0.5CH_2Cl_2, imidazole, CH_3OH.

Heating a solution of $[VOCl_2(thf)_2]$, Hcapca, and CH_3ONa (in equivalent quantities) in acetonitrile under reflux resulted in the formation of a red precipitate. The red solid was a mixture of **1** and NaCl [Eq. (1)].

$$[VOCl_2(thf)_2] + \text{Hcapca} + CH_3ONa \rightarrow \textit{trans}\text{-[VOCl(capca)]}\ (\mathbf{1}) + NaCl + CH_3OH \quad (1)$$

Soxhlet extraction of the solid with dichloromethane (3 days) gave **1**·CH_2Cl_2 in 52% yield. In an effort to increase the yield of **1**·CH_2Cl_2 and to reduce the time of the preparation, the same reaction was repeated in methanol (as a base triethylamine was used instead of sodium methoxide), for which the reaction time was ~4 h at room temperature and the yield 82%. The method of ligand substitution was employed for the preparation of compounds **2**, **3**, **4**, **5**, **6**·CH_3NO_2, and **7**. The oxovanadium(IV) compounds, with the reduced ligand H_2capcah, **8**·0.5CH_2Cl_2 (method B), **9**, **10**·2CH_3OH, **11** were prepared in a fashion similar to their capca$^-$ analogues.

Crystallography: A selection of interatomic distances and bond angles relevant to the vanadium coordination sphere for compounds **1**·CH_3OH,[29] **8**·$CHCl_3$, **9**·2CH_3CN, **10**·CH_3CN, and **12** are listed in Table 1. The vanadium atom in **8**·$CHCl_3$, has sixfold, severely distorted, octahedral coordination, with the Hcapcah$^-$ ligating atoms N_{pyr}, N_{amide}^-, and N_{amine}, and a chlorine atom forming the equatorial plane, and the oxo group and the N_{pyr} of Hcapcah$^-$ in the apical sites (Figure 1B). Of the four V–N bonds, the bond length to N2 ($d(V^{IV}–N_{amide}) = 2.019(3)$ Å), that is, the deprotonated amide nitrogen, is at the high limit of those reported in the literature for similar oxovanadium(IV)-amidate compounds.[32] The bond length to N3 (2.133(3) Å), the secondary aromatic amine nitrogen, is substantially longer (about 0.05 Å) than the V–N_{imine} bond length (2.079(6) Å) of compound **1**·CH_3OH.

The bond lengths to N1 (2.103(3) Å) and N4 (2.345(3) Å), the pyridine nitrogens, are substantially longer than the V–N2 bond length and different from each other as a consequence of the difference in the *trans* atoms (N3 and O^{2-}, respectively)

Table 1. Interatomic distances and angles relevant to the vanadium(IV) coordination sphere for **1**·CH_3OH,[a] **8**·$CHCl_3$, **9**·2CH_3CN, **10**·CH_3CN, and **12**.

	1·CH_3OH	**8**·$CHCl_3$	**9**·2CH_3CN	**10**·CH_3CN	**12**
bond lengths [Å]					
V–O2	1.626(5)	1.605(3)	1.602(2)	1.593(2)	1.592(3)
V–Cl1	2.569(3)	2.359(1)			
V–N1	2.120(7)	2.103(3)	2.103(2)	2.092(2)	2.093(3)
V–N2	2.010(7)	2.019(3)	2.010(2)	2.026(2)	2.013(3)
V–N3	2.079(6)	2.133(3)	2.118(2)	2.128(2)	2.122(4)
V–N4	2.171(7)	2.345(3)	2.357(2)	2.342(2)	2.359(3)
V–N5			2.040(2)	2.040(3)	2.105(3)
bond angles [°]					
O2-V-N2	103.1(3)	100.9(2)	99.4(1)	100.7(1)	103.9(1)
O2-V-N1	94.5(3)	102.2(1)	102.9(1)	101.0(1)	103.5(1)
N2-V-N1	78.7(3)	78.4(1)	78.6(1)	78.0(1)	78.8(1)
O2-V-N5			98.3(1)	94.9(1)	94.2(1)
N2-V-N5			162.3(1)	164.2(1)	161.9(1)
N1-V-N5			95.8(1)	96.5(1)	96.7(1)
O2-V-N3	102.0(3)	98.9(2)	97.1(1)	99.2(1)	96.2(1)
N2-V-N3	78.6(2)	80.2(1)	81.1(1)	80.1(1)	81.3(1)
N1-V-N3	154.4(3)	152.4(1)	153.4(1)	152.5(1)	154.8(1)
N5-V-N3			98.4(1)	100.2(1)	97.5(1)
O2-V-N4	90.5(3)	170.2(1)	170.5(1)	172.0(1)	167.6(1)
N2-V-N4	154.0(2)	83.3(1)	80.1(1)	82.2(1)	80.1(1)
N1-V-N4	122.8(3)	87.3(1)	86.3(1)	86.9(1)	88.8(1)
N5-V-N4			82.8(1)	82.7(1)	82.3(1)
N3-V-N4	76.9(3)	73.0(1)	73.4(1)	73.8(1)	72.6(1)
O2-V-Cl1	165.3(2)	96.2(1)			
N2-V-Cl1	90.2(2)	162.9(1)			
N1-V-Cl1	81.8(2)	96.7(1)			
N3-V-Cl1	86.6(2)	98.6(1)			

[a] From reference [29].

0947-6539/01/0712-2700 $ 17.50+.50/0 *Chem. Eur. J.* **2001**, *7*, No. 12

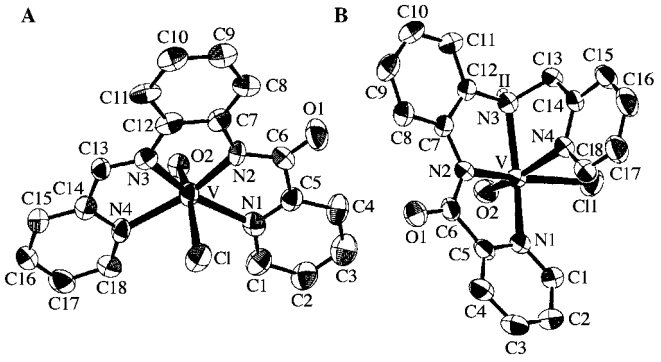

Figure 1. Structures of $\mathbf{1}\cdot CH_3OH$ (**A**) (from reference [29]) and $\mathbf{8}\cdot CHCl_3$ (**B**) showing thermal ellipsoids at 50% probability and the atom numbering scheme. For clarity hydrogen atoms are omitted.

and consistent with the literature values.[34] The V=O2 and V−Cl1 bond lengths, being 1.605(3) and 2.345(3) Å, respectively, are consistent with those found in mononuclear octahedral vanadium(IV) compounds that contain the *cis*-$V^{IV}OCl$ unit.[26, 35] The one notable difference between the X-ray crystal structure of $\mathbf{8}\cdot CHCl_3$ and $\mathbf{1}\cdot CH_3OH$ (Figure 1A) is an almost planar conformation of capca$^-$ ligand in the latter as opposed to nonplanar conformation of Hcapcah$^-$ ligand in $\mathbf{8}\cdot CHCl_3$, due to steric hindrance (vide infra). The structures of compounds $\mathbf{9}\cdot 2CH_3CN$, $\mathbf{10}\cdot CH_3CN$, and **12**, shown in Figure 2 are very similar to the structure of $\mathbf{8}\cdot CHCl_3$. At this point, it is worth noting that the vanadium–imidazole distance (2.105(3) Å) in **12** is similar to those previously reported[30d, 36] (mean $V-N_{imidazole}\sim 2.10$ Å) and the dihedral angle O2-V-N5-C19 is 27°; this means that the imidazole ring is almost parallel to V=O bond.[36b]

Electronic spectra: Table 2 lists the spectral data for the oxovanadium(IV) compounds with the ligands Hcapca and H_2capcah. Compounds **8**–**11**, the $V^{IV}O^{2+}$-Hcapcah$^-$ complexes, display two low-intensity d–d transitions at ~660–720 and ~460–510 nm. The $V^{IV}O^{2+}$–capca$^-$ compounds, except of **3** and $\mathbf{6}\cdot CH_3NO_2$,[37] display one low-intensity d–d transition at ~730–800 nm.

Infrared spectroscopy: Assignments of some diagnostic bands are given in Table 3. Differences between the spectra of the ligands Hcapca, H_2capcah, and their oxovanadium(IV) compounds are readily noticeable. The $\nu(NH)_{amide}$ band is absent in the spectra of compounds $\mathbf{1}\cdot CH_2Cl_2$–**7**, as expected from the stoichiometry. The spectrum of H_2capcah exhibits two ν(NH) bands at 3334 and 3057 cm^{-1}, in accord with the presence of two −NH− groups in its formula. The amide deprotonation in complexes **8**–**11** results in the appearance of only one band attributable to ν(NH) in these complexes. Moreover, the amide II and III bands (present in the spectra of Hcapca and H_2capcah) are replaced by a strong band at 1378–1345 cm^{-1} in compounds $\mathbf{1}\cdot CH_2Cl_2$–**11**. This replacement is to be expected as the removal of the amide proton produces a pure C–N stretch.[38] In the spectra of the complexes the ν(CO) bands appear at lower frequencies relative to the free ligand; this shift can be explained by a decrease of the double bond character of >C=O due to a considerable degree of charge delocalization of the deprotonated amide group in the complexes.

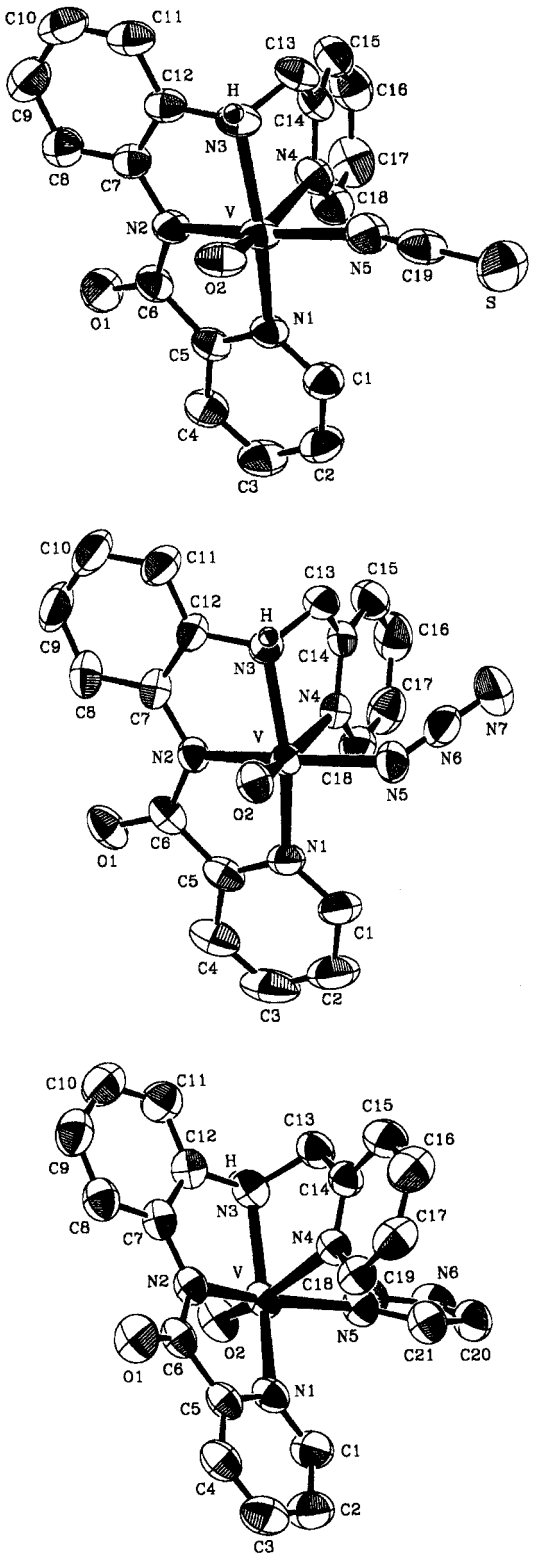

Figure 2. Structure of $\mathbf{9}\cdot 2CH_3CN$ (top), $\mathbf{10}\cdot CH_3CN$ (middle), and **12** (bottom) with thermal ellipsoids at 50% probability and the atom numbering scheme. For clarity hydrogen atoms are omitted.

The band at ~620 cm^{-1} in the free ligands, attributable to the in-plane deformation of the 2-pyridyl ring, shifts to higher

Table 2. UV/Vis spectral data for the oxovanadium(IV) compounds.

Compound	Solvent	λ_{max} [nm] (ε [$M^{-1}cm^{-1}$])
1·CH_2Cl_2	methanol	735 (48), 453 (3200), 326 (10200), 255 (sh) (7200), 228 (sh) (9000), 201 (19500)
	nitromethane	811 (71), 459 (3400)
2	methanol	732 (89), 453 (3400), 332 (11300), 254 (sh) 14800), 224 (sh) (20200), 197 (46000)
3	methanol	450 (1900), 346 (sh) (6500), 285 (11900), 274 (sh) (11600), 224 (sh) (13600), 196 (32900)
4	dichloromethane	772 (74), 418 (sh) (3800), 313 (11900), 289 (sh) (11700), 263 (14300), 219 (17200)
5	dichloromethane	766 (85), 421 (4200), 315 (14600), 259 (sh) (19000), 229 (29400), 220 (28900)
6·CH_3NO_2	methanol	451 (1900), 284 (sh) (6700), 258 (sh) (10100), 203 (63900)
7	methanol	883 (140), 266 (13500), 221 (sh) (25900), 202 (43000)
8·0.5CH_2Cl_2	methanol	721 (35), 479 (sh) (67), 285 (sh) (6800), 261 (13500), 206 (24500)
9	acetonitrile	686 (45), 498 (56), 354 (sh) (3400), 307 (sh) (6500), 285 (sh) (7500), 262 (14150), 225 (sh) (20200), 200 (42400)
	nitromethane	694 (43), 516 (sh) (105)
10·2CH_3OH	acetonitrile	705 (150), 502 (sh) (245), 287 (sh) (9800), 262 (16800), 202 (42600)
	methanol	661 (sh) (50), 458 (sh) (240), 285 (sh) (6700), 260 (11400), 200 (39900)
11	methanol	702 (38), 459 (sh) (210), 285 (sh) (6000), 260 (9600), 201 (33200)

Table 3. Diagnostic infrared bands [cm^{-1}] of the ligands Hcapca and H_2capcah, and their oxovanadium(IV) compounds.

	ν(NH)	ν(CO)	amide II[b]	ν(C-N)$_{amide}$	amide III[b]	ν(V=O)	δ(py)[c]	ν(V-X)[d]
Hcapca	3283 (m)	1686 (vs)[a]	1534 (vs)		1277 (m)		619 (m)	
1·CH_2Cl_2		1636 (vs)		1353 (s)		955 (s)	652 (w)	
2		1648 (vs)		1346 (vs)		958 (vs)	654 (w)	2070 (vs)[e]
3		1636 (s)		1349 (s)		944 (s)	656 (w)	2051s[f],2036 (vs)[f]
4		1629 (vs)		1349 (vs)		939 (s)	651 (m)	1598s[g],1383 (m)[h]
5		1648 (vs)		1345 (vs)		941 (vs)	650 (w)	1600 (vs)[g],1362s[h]
6·CH_3NO_2		1619 (s)		1378 (s)		966 (vs)	660 (m)	
7		1638 (vs)		1363 (vs)		968 (vs)	656 (w)	
H_2capcah	3334s, 3057 (w)	1661 (vs)[a]	1520 (vs)		1272 (m)		622 (m)	
8·0.5CH_2Cl_2	3140 (m)[e]	1638 (vs)		1369 (vs)		973 (vs)	655 (m)	392 (m)[i]
9	3067 (m)	1624 (s)		1376 (s)		973 (vs)	655 (m)	2061 (vs)[e]
10·2CH_3OH	3065 (m)	1636 (s)		1371 (s)		966 (s)	653 (m)	2069 (vs)[f]
11	3125 (w)	1630 (s)		1371 (s)		972 (s)	660 (m)	

[a] ν(C=O). In secondary amides this vibration is called amide I. [b] In secondary amides, these bands arise from coupled ν(CN) and δ(NH) modes. [c] In-plane pyridine ring deformation. [d] Where X = Cl^-, NCS^-, N_3^-, CH_3COO^-, $C_6H_5COO^-$. [e] $\nu(CN)_{isothiocyanate}$. [f] $\nu_{as}(NNN)$. [g] $\nu_{as}(CO_2^-)$. [h] $\nu_s(CO_2^-)$. [i] ν(V–Cl).

frequencies in the spectra of the vanadium complexes; this indicates[39] that the pyridine nitrogen atoms of capca$^-$ and Hcapcah$^-$ coordinate to V^{IV}.

The V=O stretching frequency in complexes **1**·CH_2Cl_2–**5**, which contain the *trans*-[V(=O)X] unit (X = monoanionic ligand), ranges from 939 to 955 cm^{-1}; this band appears at ~970 cm^{-1} in complexes **6**–**11**, which contain a neutral ligand *trans* to the oxo group. From these IR data, it is reasonable to assume that the presence of an anionic ligand *trans* to O^{2-} weakens the V=O bond.

The spectra of **2** and **9** exhibit the ν(CN) mode in the region characteristic of terminal N-bonded thiocyanate groups.[40] The spectra of **3** and **10**·2CH_3OH exhibit very strong bands in the 2036–2069 cm^{-1} range, assignable to the antisymmetric stretching vibration of the coordinated azido ligand;[40] the splitting of this band in **2** is probably a consequence of crystal site effects. The higher frequency of the $\nu_{as}(N_3)$ mode in **10**·2CH_3OH relative to that in **3** indicates a larger difference between the two N–N distances in the former.[41] The parameter Δ [$\Delta = \nu_{as}(CO_2) - \nu_s(CO_2)$] for **4** (215 cm^{-1}) and **5** (238 cm^{-1}) is larger than that for NaO_2CCH_3 (164 cm^{-1}) and NaO_2CPh (184 cm^{-1}), respectively, as expected for the proposed monodentate coordination of the carboxylate ligands.[40, 42]

Theoretical calculations on *cis*-[VOCl(Hcapcah)]: To get an insight into the structure of compound *cis*-[VOCl(Hcapcah)]·$CHCl_3$ (**8**·$CHCl_3$), a series of theoretical calculations were performed in order to search for other minima in the potential energy surface of the complex. Because of the high number of atoms, and with the aim to speed up the calculations, the analysis was undertaken by using a model in which, the Hcapcah$^-$ ligand was replaced by the model ligand [HN=CH-CH_2-NH-CH=CH-N-C(O)-CH=NH]$^-$ (L^-) which has the same donor atoms and reproduces the conjugated system of the actual ligand well.

The ab initio study started from the optimization of a series of low-energy conformers of the model complex [VOCl(L)];

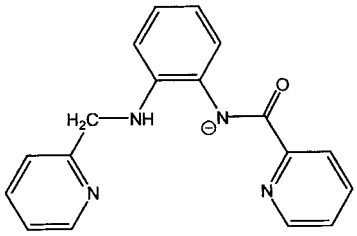

Hcapca$^-$

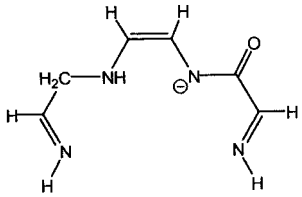

L^-

0947-6539/01/0712-2702 $ 17.50+.50/0 *Chem. Eur. J.* **2001**, *7*, No. 12

this was accomplished through the choice of the starting geometry of the optimization process namely the model **M1**, derived from the X-ray structure of *cis*-[VOCl(Hcapcah)], the model **M2** also derived from the X-ray structure but with the O^{2-} and Cl^- ligands interchanged, and finally the model **M3**, in which upon rotation around the $-CH_2-NH-$ single bond the model ligand has its four nitrogen donor atoms in the basal plane of the complex and the [VOCl] moiety in a *trans* arrangement. The final optimized geometries of these model isomers are depicted in Figure 3, while selected structural parameters are reported in Table 4. For the sake of comparison, the experimental data are also included in the table. All isomers are minima in the potential surface of the model as calculation of the Hessian gave no imaginary frequencies in all cases. The scaled ν(V=O) stretching frequency has been calculated equal to 951 cm^{-1} for **M1**, that is, very close to the experimental value of 973 cm^{-1}, whereas the ν(V=O) calculated frequencies for **M2** and **M3** were 921 and 931 cm^{-1} respectively. In general, and taking into account that the model is simplified and surely less hindered, one can observe quite a satisfactory agreement between the **M1**

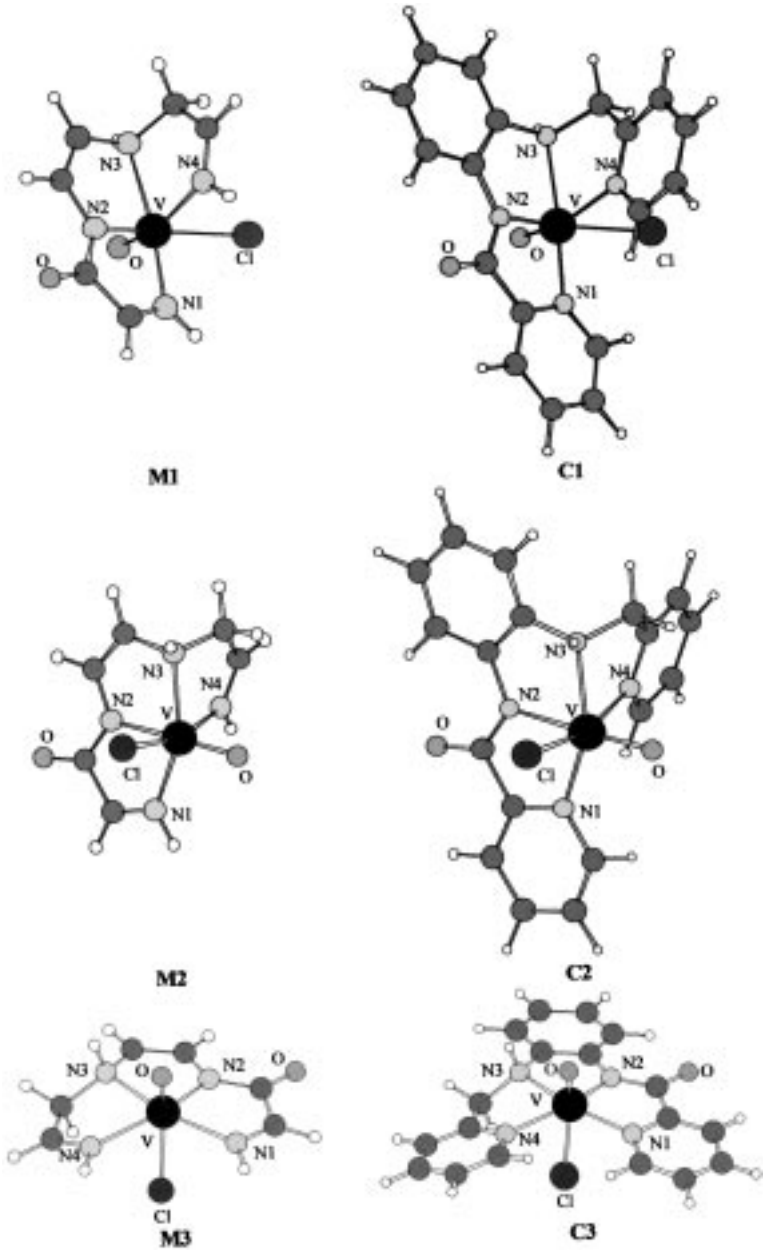

Figure 3. Final optimized geometries of the isomers of the [VOCl(L)] model complex (**M1**, **M2**, and **M3**) and [VOCl(Hcapcah)] compound (**C1**, **C2**, and **C3**).

Table 4. Selected bond lengths [Å] and angles [°] calculated for the isomers of the [VOCl(L)] model and the [VOCl(Hcapcah)] complex.[a]

	M1	M2	M3	C1	C2	C3	Exptl
V–Cl1	2.406	2.361	2.550	2.404	2.371	2.543	2.358
V–O2	1.602	1.618	1.613	1.602	1.620	1.614	1.605
V–N1	2.090	2.079	2.119	2.092	2.086	2.116	2.103
V–N2	2.020	2.130	1.997	2.017	2.127	2.000	2.019
V–N3	2.217	2.180	2.166	2.155	2.139	2.138	2.133
V–N4	2.303	2.151	2.161	2.366	2.177	2.191	2.346
O2-V-Cl1	99.9	102.6	160.3	98.6	101.6	161.5	96.2
N1-V-N2	77.1	74.5	77.5	79.3	76.6	79.7	78.4
N2-V-N3	80.1	78.2	79.8	81.5	79.2	81.1	80.2
N3-V-N4	71.7	75.3	75.8	73.1	77.0	76.5	73.5

[a] Numbering scheme as in Figure 1.

model and the experimental values of geometrical parameters. Bond lengths agree within 0.08 Å, while the largest deviation of bond angles appears to be about 4°. Concerning the energetics of the system, the **M1** isomer is found to be the global minimum, whereas **M2** and **M3** isomers have been found to be 17.8 and 20.2 kJ mol^{-1} higher in energy.

Having located the three minima, by using the model calculations, we proceeded to the theoretical study of the actual *cis*-[VOCl(Hcapcah)] complex. We optimized in the same level of theory the isomer **C1**, which is based on the X-ray structure, and the isomers **C2** and **C3**, which were built by using models **M2** and **M3**, respectively. The final optimized geometries of these isomers are shown in Figure 3, while selected structural parameters are given in Table 4. All isomers are minima in the potential surface of the model as frequency calculations gave only real frequencies in all cases. There is apparently a better agreement between the calculated geometry **C1** with that found experimentally, compared with that found for the model **M1**. The largest deviation of bond lengths is about 0.05 Å, while that of bond angles is about 2°. The **C1** isomer corresponding to the experimental structure is found to be the more stable one, whereas **C2** and **C3** isomers have been found to be 20.0 and 28.4 kJ mol^{-1} higher in energy, respectively.

An interesting structural aspect of the isomers calculated in this theoretical study, concerns the high energy of isomeric structures **M3** and **C3**. In both structures the macrocyclic ligand adopts a quasi-planar conformation; this implies an apparent deformation energy in relation to the most stable conformation of the ligand found in the other isomers of the complex. A further destabilization results from the *trans* orientation of the oxo and chlorine ligands in the {V^{IV}(=O)-(Cl)} fragment. Calculations at the same level of theory show that the *trans*-{V^{IV}(=O)(Cl)}$^+$ fragment is 15.8 kJ mol^{-1} higher in energy than the *cis*-{V^{IV}(=O)(Cl)}$^+$ one. Thus, the *trans* **M3** and **C3** structures are destabilized by 20.2 and 28.4 kJ mol^{-1} in relation to the global minima **C1** and **M1**, respectively.

In the X-ray structure of *cis*-[VOCl(Hcapcah)] there is an apparent *trans* influence induced by the oxo group. Thus, the V−N4 bond length (2.345(3) Å) is found to be significantly stressed with respect to a normal V−N bonds (mean value 2.085 Å). This *trans* influence is reproduced nicely by the the theoretical calculations. In the optimized structure **C1**, the V−N4 distance is 2.366 Å and the calculated mean value for the other three V−N bonds is 2.088 Å. In the case of the **C3** isomer, the calculated V−Cl1 bond length, *trans* to the oxo group, is found to be 0.14 to 0.17 Å longer than the V−Cl1 bond length in **C1** and **C2**, which contain the *cis*-{V^{IV}(=O)-(Cl)} unit.

Magnetism and electron paramagnetic resonance spectra: The magnetic moments of compounds **1**·CH_2Cl_2 – **11** are in the range 1.64 – 1.81 μ_B (see Experimental Section) at 298 K, in accord with the spin-only value expected for d^1 $S = ½$ systems. The EPR parameters (***A*** and ***g*** tensors) of the severely distorted octahedral V^{IV}O^{2+} compounds, with a weak sixth ligand *trans* to the oxo group, were determined by computer simulation of the experimental EPR spectra and are reported in Table 5. The EPR spectra of the oxovanadium(IV) compounds are typical of monomeric V^{IV}O^{2+} ($S = ½$, $I = 7/2$) species with no evidence for magnetic couplings between electron spins, that is, line-broadening or splittings in the spectral features.

The equatorial ligands in compounds **1**·CH_3OH (and **1**·CH_2Cl_2 as well) and **2** – **7** were studied by electron spin-echo envelope modulation (ESEEM) spectroscopy.[43] ESEEM is a pulsed EPR technique, eminently suited for measuring weak hyperfine couplings. Orientation-selective ESEEM spectra recorded across the EPR spectrum of compound **1**·CH_3OH were dominated by two sets of sharp features at 3 – 5 MHz and 7 – 9.5 MHz. According to numerical simulations, performed as described in reference [44], the ESEEM spectra are assigned to $^{14}N(I = 1)$ nuclei coupled to the electron spin $S = 1/2$. Two classes of almost isotropic ^{14}N hyperfine couplings were resolved, with A_{iso} values of 5.2 and 6.1 MHz, respectively. These couplings are typical for $^{14}N(I = 1)$ atoms equatorially coordinated to V^{IV}O^{2+}. The ESEEM spectra recorded for **2** – **7** are comparable to those for **1**·CH_3OH and this indicates that the equatorial coordination environment for compounds **2** – **7** is similar to the equatorial environment of **1**·CH_3OH, that is, an N_4 donor-atom set for all complexes. Moreover, the ESEEM spectra show that in all four cases the $^{14}N(I = 1)$ hyperfine couplings are comparable, and this means that the bonding properties of the equatorial ligands in compounds **1**·CH_3OH and **2** – **7** are similar.

Figure 4 displays a correlation plot, between A_z and g_z values for a series of known oxovanadium(IV) compounds (open circles) with various equatorial-donor-atom sets (Cl_4,[26]

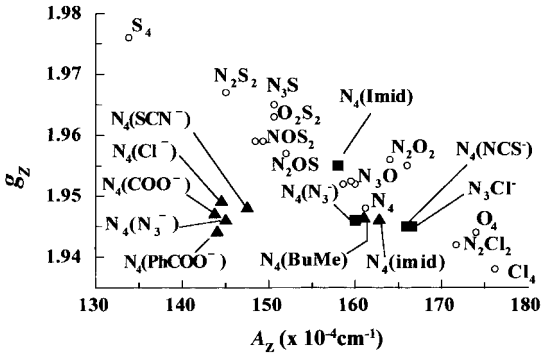

Figure 4. A correlation plot of g_z versus A_z for the V^{IV}O^{2+} compounds **1** – **7** (◆), **8** – **11** (■), and a series of known oxovanadium(IV) compounds (○) with various equatorial donor atoms.

O_4,[45] N_2Cl_2,[26] N_2O_2,[45] N_4,[46] N_3O,[26, 47] N_2OS,[26] NOS_2,[26] O_2S_2,[48] N_3S,[32c] N_2S_2,[49] and S_4[50]). Addition of the g_z and A_z values for **1**·CH_2Cl_2 – **11** to this plot reveals that: i) the points of compounds **1** – **5**, with anionic axial ligands, deviate substantially from the locus of the correlation line, due to their lower (~10%) A_z values relative to reference (V^{IV}O)N_4 compounds and ii) the points of compounds **6** – **11**, with neutral axial ligands, fall on the main locus of the line.

Apart from the g_z versus A_z correlation, the observed A_z values can be discussed on the basis of the empirical "additivity relationship".[8, 26] Application of the additivity relationship for compounds **1**·CH_2Cl_2 – **7** gives a calculated A_z value[51] of 161 × 10^{-4} cm^{-1} with proposed equatorial coordi-

  0947-6539/01/0712-2704 $ 17.50+.50/0 *Chem. Eur. J.* **2001**, *7*, No. 12

Table 5. EPR parameters for the oxovanadium(IV) compounds.[a]

Compound	Solvent	g_x[b]	g_y[b]	g_z[b]	10^{-4} cm^{-1} A_x[b]	A_y[b]	A_z[b]
1 · CH_2Cl_2[c]	CH_3OH[d]	1.981	1.979	1.947	53.0	49.0	145.0
	H_2Cl_2	1.980	1.980	1.947	53.0	50.0	145.5
	H_3NO_2	1.981	1.980	1.947	53.0	49.0	145.5
	H_3CN	1.981	1.980	1.947	53.0	49.0	145.5
	DMF	1.98	1.98	1.948	51	51	145
2	CH_3OH[d]	1.981	1.980	1.948	52.0	48.0	147.5
	H_3NO_2	1.981	1.979	1.947	52.0	48.0	148.0
3	CH_3OH[d]	1.984	1.980	1.949	52.0	45.0	144.5
	H_3CN	1.984	1.980	1.949	52.0	45.0	144.5
	H_3NO_2	1.981	1.979	1.947	53.0	49.0	145.0
4	CH_3OH[d]	1.982	1.978	1.946	52.0	49.0	145.0
	CH_3NO_2	1.984	1.981	1.948	52.0	50.0	144.5
5	CH_3OH[d]	1.982	1.980	1.944	54.0	49.0	144.0
	CH_3CN	1.982	1.980	1.944	54.0	49.0	144.0
6 · CH_3NO_2	CH_3OH[d]	1.981	1.979	1.947	56.0	55.0	162.5
	CH_2Cl_2	1.981	1.979	1.947	56.0	55.0	162.5
	CH_3NO_2	1.980	1.978	1.946	58.0	55.0	162.0
	DMF	1.98	1.98	1.46	58	58	162.0
	powder	–	–	1.46 – 1.48	–	–	160 – 62
7	CH_3OH[d]	1.980	1.978	1.946	58.0	55.0	162.0
	CH_3CN	1.980	1.978	1.946	58.0	55.0	162.0
8 · 0.5 CH_2Cl_2	CH_3OH[d]	1.984	1.981	1.946	58.0	54.0	163.0
	CH_3NO_2	1.984	1.980	1.945	59.0	55.0	166.0
9	CH_3OH[d]	1.982	1.981	1.946	56.0	56.0	160.0
	CH_3NO_2	1.982	1.981	1.946	56.0	56.0	160.0
10 · 2 CH_3OH	CH_3OH[d]	1.983	1.980	1.946	58.0	55.0	163.0
	CH_3NO_2	1.982	1.980	1.945	58.0	55.0	166.0
11	CH_3OH[d]	1.987	1.987	1.955	58.0	55.0	158.0
	CH_3NO_2	1.987	1.987	1.955	58.0	55.0	158.0

[a] A variety of solvents was used to run the cw EPR spectra of the oxovanadium(IV) compounds in order to prove that their $g_{x,y,z}$ and $A_{x,y,z}$ values were independent of the solvent. [b] Errors: g values ± 0.002, $A_{x,y,z}$ values $\pm 0.5 \times 10^{-4}$ cm^{-1}. [c] We ran the cw EPR spectra of the crystalline material **1** · CH_3OH in the solvents CH_3OH, CH_2Cl_2, CH_3NO_2, CH_3CN, and DMF; the cw EPR parameters were exactly the as those of **1** · CH_2Cl_2 in the corresponding solvents. [d] Thoughout the whole paper the EPR values of **1**–**11** taken in methanol are those reported/used.

nation (2_{pyr}, 1−CO*N*$^-$, 1−N=(aliphatic amine)), while for compounds[51] **8** · 0.5 CH_2Cl_2, **9**, and **11** calculated observed A_z values of 160, 159, and 157 $\times 10^{-4}$ cm^{-1}, respectively, are found with proposed equatorial coordination ($1N_{pyr}$, 1−CO*N*$^-$, 1−NH, 1X; X = Cl$^-$, NCS$^-$, and imidazole for compounds **8** · 0.5 CH_2Cl_2, **9**, and **11** respectively). From this analysis, it is evident that using the additivity relationship one can reasonably predict the equatorial-donor-atom groups *only* for the compounds **6**–**11**, that is, those following the expected g_z versus A_z correlation. For compounds **1** · CH_2Cl_2–**5** the measured A_z values are between 144 – 145 ' 10^{-4} cm^{-1}, that is, ~10% less than the expected values for N_4 reference $V^{IV}O^{2+}$ compounds. Such low experimental A_z values cannot result from any combination of published A_z contributions for the types of nitrogen atoms of the capca$^-$, but rather fall in the range at which sulfur contributions are expected. Thus, it becomes crystal-clear that for the compounds **1** · CH_2Cl_2–**5**, that is, those not following the expected g_z versus A_z correlation the use of the additivity relationship can result in misleading conclusions about the coordination environment of vanadium. On the other hand, taking into account the g_z versus A_z correlation plot is a practical rule to possibly avoid such problems.

Interpretation of the reduced A_z values for *trans*-[V^{IV}(=O)-(X$^-$)] compounds: The ^{51}V hyperfine coupling parameters, neglecting small terms, can be expressed in the form of Equations (2a) – (2c) ($\Delta g_{x,y,z} = (g_e - g_{x,y,z})$.[52]

$$|A_z| = |-P[K + 4/7\,c^2 + \Delta g_z + 3/14(\Delta g_x + \Delta g_y)]| \quad (2a)$$

$$|A_x| = |-P[K - 2/7\,c^2 + \Delta g_x - 3/14\,\Delta g_y]| \quad (2b)$$

$$|A_y| = |-P[K - 2/7\,c^2 + \Delta g_y - 3/14\,\Delta g_x]| \quad (2c)$$

$$P = g_n\beta_n g\beta_e\langle r^{-3}\rangle \quad (2d)$$

P is the dipolar interaction between the unpaired d electron and the ^{51}V nucleus and is determined by the spatial distribution of the d electron.[52] K is the Fermi contact term and is a measure of the unpaired s-electron spin density at the nucleus, which is influenced by the polarization of the inner s electrons by interaction with the unpaired d electron.[27, 51] The factor $(\beta_2^*)^2$ is, to a good approximation, the population of the ground-state d orbital where the unpaired spin is localized. For oxovanadium(IV) complexes with C_{2v} symmetry or higher, $(\beta_2^*)^2$ gives the population of the d_{xy} orbital.[27, 52, 53]

From Equations (2a) – (2c), we obtain Equations (3a) and (3b):

$$|A_z| - |(A_x + A_y)/2| = |P[6/7\,(\beta^*)^2 + \Delta g_z - 5/28\,(\Delta g_x + \Delta g_y)]| \quad (3a)$$

$$\Rightarrow |A_z| = |P[6/7\,(\beta^*)^2 + \Delta g_z - 5/28\,(\Delta g_x + \Delta g_y)]| + |(A_x + A_y)/2| \quad (3b)$$

In Equation (3), $(\beta^*)^2$ is used to indicate that the unpaired d electron resides mainly on the d_{xy} orbital.

From Table 5 we see that for the compounds **1**·CH_2Cl_2–**7** the differences in the g values are small, namely: <0.04 for the g_z and <0.005 for the $g_{x,y}$ values, while the differences in the average $(A_x+A_y)/2$ values do not exceed 4×10^{-4} cm^{-1}. Under these conditions, according to Equation (3b) the observed changes in the A_z values between compounds **1**·CH_2Cl_2–**5**, and **6** and **7** originates from two possible mechanisms, which imply either changes in the $(\beta^*)^2$ values, that is, the covalency of the unpaired electron, or changes in the values of the dipolar parameter P. The relative impact of these parameters can be visualized by plotting the A_z values calculated according to Equation (3b) for a range of pertinent values of P and $(\beta^*)^2$. Such a plot is displayed in Figure 5, for which,

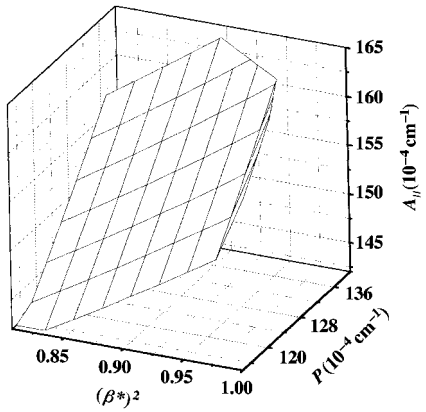

Figure 5. Dependence of the A_z values on the electron–nuclear dipolar coupling constant P, and the population of the ground state nonbonding orbital $(\beta^*)^2$. The data points have been calculated by using Equation (3b). Other values are: $\Delta g_{x,y}=0.005$, $(A_x+A_y)/2=55\times10^{-4}$ cm^{-1}. For a given P value, reduction of the $(\beta^*)^2$ value leads to a decrease of the A_z values. On the other hand for a given set of equatorial donor atoms, that is, a given $(\beta^*)^2$ value, a decrease in the value of P leads to a reduction of the A_z.

based on Table 5, we have used $\Delta g_{x,y}$ values of 0.005 and an average $(A_x+A_y)/2$ of 55×10^{-4} cm^{-1}. Prior to the discussion of the present results, some general comments concerning this plot are in due. For a given P value, reduction of the $(\beta^*)^2$ value leads to a decrease of the A_z values (Figure 5). This is actually the origin of the correlation between g_z versus A_z, as discussed earlier in the present paper. On the other hand for a given set of equatorial donor atoms, that is, a given $(\beta^*)^2$ value, a decrease in the value of P leads to a reduction of A_z.

Our data, presented in the preceding paragraphs, show that in **1**·CH_2Cl_2–**5**, and in **6** and **7** the equatorial ligands remain invariant. Therefore, we assume that the value of $(\beta^*)^2$ should not vary by much between in these compounds. In Figure 5 the data for these compounds correspond to a $(\beta^*)^2$ value of 0.9, which is a reasonable value for an oxovanadium(IV) compound with an N_4 equatorial-donor-atom set.[26] In this context, the reduction of A_z from 162×10^{-4} cm^{-1}, observed for **6**·CH_3NO_2 and **7**, to 144×10^{-4} cm^{-1}, observed for **1**·CH_2Cl_2, corresponds to a reduction of the P value by 23×10^{-4} cm^{-1}, that is, $\sim16\%$. Therefore, we suggest that the observed reduction of A_z values in *trans*-[V(=O)X$^-$] compounds can be fully accounted for by a reduction of the P value by $\sim16\%$.

According to Equation (2d) a reduced P value implies a larger $\langle r^{-3}\rangle$ value, which physically means a radial expansion of the $3d_{xy}$ orbital and a reduced electron density on the metal.[27, 54] This reduced electron density is expected to result in a decreased V=O bond strength.[27, 55] From Tables 3 and 5, it is seen that the lower A_z values are correlated with reduced ν(V=O) frequencies, and this can be taken as evidence for the validity of the assumed mechanism.

Conclusion

The design and synthesis of the tetradentate amidate ligand Hcapca, with conjugated double bonds and a maximum equatorial charge of -1 upon ligation to a vanadium atom, allowed us to prepare a series of unprecedented *trans*-$[V^{IV}OX(capca)]^{0/+}$ compounds, with either monoanionic or neutral axial ligands. Reduction of Hcapca breaks the double-bond conjugation and results in the isolation of a more flexible ligand, H_2capcah, enabling us to prepare another series of *cis*-$[V^{IV}OX(Hcapcah)]^{0/+}$ compounds with only *neutral* axial ligands, that is, the pyridine nitrogen atom of Hcapcah$^-$. The *cis*/*trans*-oxovanadium(IV) compounds were structurally and spectroscopically (mainly by cw EPR) characterized. Through these two series of oxovanadium(IV) compounds, which contain very similar tetradentate ligands, we were able to investigate the effect of the charged axial ligands on the ^{51}V hyperfine coupling constants and in particular on the parallel component, A_z.

The main effect of the monoanionic axial ligands on the ^{51}V hyperfine coupling constants is the reduction of the A_z values by almost 10% compared to N_4 reference complexes. The z component of the $^{51}V(I=7/2)$ hyperfine coupling tensor A, has been extensively employed as a benchmark for the identification of the equatorial-donor-atom sets in oxovanadium(IV) complexes. Therefore, the present data reveal a novel phenomenon which bears strong relevance to the use of the A_z value as predictive tool in vanadoproteins or $V^{IV}O^{2+}$-substituted proteins and oxovanadium(IV) model compounds. This means that in certain cases, factors other than the equatorial-donor-atom sets, that is, axial charge, may result in significant variations of the A_z values of $V^{IV}O^{2+}$ compounds. Such exceptional cases can be traced from the deviation of the pertinent points in a g_z versus A_z correlation plot.

The reduced A_z and ν(V=O) values observed in the *trans*-$[V^{IV}(=O)X^-]$ compounds can both be explained by a simple model: the negative axial charge induces a radial expansion of the $3d_{xy}$ orbital; this results in a reduced electron density on the metal, manifested as reduced P values and lowered ν(V=O) frequencies. The $(\beta^*)^2$ values are not essentially influenced neither are the energies of the excited states, and this is consistent with the small variations in the g values, which mainly depend on the population of the low-lying excited states and their energy difference from the ground state.

Ab initio calculations on both model and actual complexes have shown that there are three isomers of the $[V^{IV}OCl$-

  0947-6539/01/0712-2706 $ 17.50+.50/0 *Chem. Eur. J.* **2001**, *7*, No. 12

(Hcapcah)] (as $\mathbf{8}\cdot CHCl_3$) complex, two with a *cis* arrangement of the {V^{IV}(=O)(Cl)} fragment and one with a *trans*-{V^{IV}(=O)(Cl)} unit. The calculated geometry of the most stable *cis* isomer agrees well with the experimental data.

Experimental Section

Materials: Reagent grade chemicals were obtained from Aldrich and used without further purification. Dichlorobis(tetrahydrofuran)oxovanadium(IV), $[VOCl_2(thf)_2]$,[56] and *N*-{2-[2-pyridylmethylene)amino]phenyl}pyridine-2-carboxamide (Hcapca),[32c] were prepared by literature procedures. The purity of the above molecules was confirmed by elemental analyses (C, H, N, and V, for vanadium compounds) and infrared spectroscopy. Merck silica gel 60F254 TLC plates were used for thin layer chromatography. Reagent grade dichloromethane, chloroform, acetonitrile, nitromethane, and thiethylamine were dried and distilled over calcium hydride, while diethyl ether was dried and distilled over sodium wire. Methanol was dried by heating under reflux over magnesium methoxide. Synthesis, distillations, crystallization of the complexes, and spectroscopic characterization were performed under high-purity argon using standard Schlenk techniques. C, H, N and S analyses were conducted by the University of Ioannina's microanalytical service; vanadium was determined gravimetrically as vanadium pentoxide or by atomic absorption, and chloride analyses were carried out by potentiometric titration. Et_4NSCN and Et_4NN_3 were synthesized as follows: an equivalent of Et_4NCl to a stirred suspension of KSCN or NaN_3 in methanol was added, and the reaction mixture was stirred overnight. The mixture was evaporated to dryness, and the residue was extracted with acetonitrile and then filtered off. The volume of the filtrate was reduced to 1/3 and a white precipitate was formed in yield ~60% for both cases.

***N*-{2-[(Pyridylmethyl)amino]phenyl}pyridine-2-carboxamide (H_2capcah)**: Hcapca (3.0 g, 9.92 mmol) was dissolved in ethanol (30 mL) and an hydrogenation catalyst (10% Pd on activated carbon, 0.60 g) was added to the mixture. Pure hydrogen was bubbled through the solution for 4 h, while the mixture with vigorously stirred by a magnet. The reaction product was separated from the catalyst by filtration, and the filtrate was evaporated to dryness to yield a yellow oil. The oil was treated with diethyl ether (20 mL) heated under reflux, yielding 2.41 g (80%) of light yellow solid. M.p. 104–105 °C; MS (70 ev): *m/z* (%): 304 (70) $[M]^+$; R_f 0.07 (4:1 chloroform/*n*-haxane); ^{1}H NMR (400 MHz, $CDCl_3$, 24 °C): $\delta = 4.56$ (s, 2H), 6.72 (d, 1H), 6.82 (t, 1H), 7.18 (t, 1H), 7.43 (d, 1H), 7.55 (d, 1H), 7.64 (t, 1H), 7.90 (t, 1H), 8.26 (d, 1H), 8.63 (d, 1H), 9.95 (s, 1H); ^{13}C{^{1}H} NMR (100.6 MHz, $CDCl_3$, 24 °C): $\delta = 49.6$, 113.58, 118.47, 121.49, 122.54, 124.19, 124.11, 126.43, 127.04, 136.95, 137.57, 141.66, 148.15, 148.89, 149.80, 158.81, 162.80; elemental analysis calcd (%) for $C_{18}H_{16}N_4O$ (304.35): C 71.03, H 5.30, N 18.40; found C 70.97, H 5.58, N 18.30.

[VOCl(capca)]$\cdot CH_2Cl_2$ ($\mathbf{1}\cdot CH_2Cl_2$)

Method A: Solid Hcapca (0.857 g, 2.84 mmol) in one portion and solid sodium methoxide (0.153 g, 2.84 mmol) in one portion were successively added to a stirred solution of $[VOCl_2(thf)_2]$ (0.80 g, 2.84 mmol) in acetonitrile (25 mL). Immediately upon addition of these materials, the color of the solution changed from blue to brown-green, and a light brown precipitate was formed. The mixture was heated under reflux for 24 h, upon which a red solid was formed with a brown-red supernatant. The reaction mixture was cooled to room temperature (15 °C), and the dark red solid was filtered off, washed with diethyl ether (10 mL), and dried in vacuo. The dark red solid was placed in a Soxhlet thimble and extracted with dichlorometnane (~60 mL) for 3 days. The volume of the filtrate (50 mL), which already contained a red precipitate, was reduced in vacuum to about 10 mL and then allowed to −20 °C. After 24 h the precipitate was filtered off, washed with diethyl ether (2 × 10 mL), and dried in vacuo to afford 0.72 g of $\mathbf{1}\cdot CH_2Cl_2$ (52%). Elemental analysis calcd (%) for $C_{19}H_{15}Cl_3N_4O_2V$ (488.64): C 46.70, H 3.09, Cl 7.25, N 11.46, V 10.42; found C 46.60, H 3.28, Cl 7.10, N 11.40, V 10.52; $\mu_{eff} = 1.71\ \mu_B$ at 298 K. Crystals of $\mathbf{1}\cdot CH_3OH$ suitable for X-ray structure analysis were obtained by vapour diffusion of diethyl ether into a concentrated solution of $\mathbf{1}\cdot CH_2Cl_2$ in methanol (at 4 °C).

Method B: Solid Hcapca (1.82 g, 6.02 mmol) was added in one portion to a stirred solution of $[VOCl_2(thf)_2]$ (1.70 g, 6.02 mmol) in methanol (7 mL). Upon addition of the ligand the blue solution changed to deep red. Then, triethylamine (0.067 g, 6.62 mmol) was added to the solution. After 20 min of stirring with a magntic stirrer a deep red solid was formed. The reaction mixture was stirred for 4 hours before being filtered, and the precipitate was washed with dichloromethane (3 × 10 mL) and dried under vacuum to yield 2.40 g of product (82%).

[VO(SCN)(capca)] (2): Solid Et_4NSCN (0.11 g, 0.59 mmol) was added to a stirred suspension of $\mathbf{1}\cdot CH_2Cl_2$ (0.29 g, 0.59 mmol) in methanol (5 mL). Upon addition of Et_4NSCN, $\mathbf{1}\cdot CH_2Cl_2$ dissolved, a brick-red precipitate was formed and solution turned from red to faint yellow. The mixture was stirred for 2 h and filtered, and the brick-red compound washed with methanol (2 × 5 mL) and diethyl ether (2 × 5 mL), and dried under vacuum to afford 0.18 g of **2** (72%). Elemental analysis calcd (%) for $C_{19}H_{13}N_5O_2SV$ (426.35): C 53.52, H 3.07, N 16.42, S 7.52, V 11.95; found C 53.20, H 3.14, N 16.32, S 7.65, V 12.05; $\mu_{eff} = 1.66\ \mu_B$ at 298 K.

[VO(N_3)(capca)] (3): Compound **3** was prepared in a fashion similar to that for complex **2** except that i) acetonitrile was used as solvent and ii) Et_4NN_3 was used instead of Et_4NSCN. The product was obtained in 64% yield. Elemental analysis calcd (%) for $C_{18}H_{13}N_7O_2V$ (410.29): C 52.69, H 3.19, N 23.89, V 1241; found C 52.90, H 3.27, N 23.75, V 12.34; $\mu_{eff} = 1.65\ \mu_B$ at 298 K.

[VO(CH_3COO)(capca)] (4): Acetic acid (0.01 g, 0.17 mmol) and triethylamine (0.017 g, mmol) were added to acetonitrile solution (4 mL), and the solution was stirred for 1.5 h. Then, the solution was cooled to 0 °C and solid $\mathbf{1}\cdot CH_2Cl_2$ (0.085 g, 0.17 mmol) was added to it in one portion. The mixture was stirred for 3 h upon which an organge-yellow precipitate was formed. The solid was filtered off, washed with acetonitrile (5 mL) and diethyl ether (2 × 5 mL), and dried under vacuum to yield 0.050 g of **4** (70%). Elemental analysis calcd (%) for $C_{20}H_{16}N_4O_4V$ (427.31): C 56.21, H 3.77, N 13.09, V 11.92; found C 55.92, H 3.73, N 13.14, V 12.01; $\mu_{eff} = 1.68\ \mu_B$ at 298 K.

[VO(PhCOO)(capca)] (5): The same procedure as for compound **4** was followed to prepare the complex, except that benzoic acid was used instead of acetic acid. The isolated yield was 62%. Elemental analysis calcd (%) for $C_{27}H_{18}N_4O_4V$ (489.38): C 61.36, H 3.70, N 10.92, V 10.41; found C 60.85, H 3.64, N 11.22, V 10.35; $\mu_{eff} = 1.81\ \mu_B$ at 298 K.

[VO(capca)(imidazole)]Cl$\cdot CH_3NO_2$ ($\mathbf{6}\cdot CH_3NO_2$): Imidazole (0.015 g, 0.22 mmol) was added to a stirred suspension of $\mathbf{1}\cdot CH_2Cl_2$ (0.110 g, 0.22 mmol) in nitromethane (10 mL). The mixture was stirred for 3 h, and a brown precipitate was formed. The solid was filtered off, washed with diethyl ether (2 × 10 mL), and dried under vacuum, yielding 0.096 g of product (80%). Elemental analysis calcd (%) for $C_{22}H_{20}ClN_7O_4V$ (532.83): C 49.59, H 3.78, N 18.40, V 9.56; found C 50.42, H 3.78, N 18.22, V 9.65; $\mu_{eff} = 1.82\ \mu_B$ at 298 K.

[VO(capca)(η-*n*BuNH_2)]Cl (7): *n*-Butylamine (0.021 g, 0.29 mmol) was added to a stirred suspension of $\mathbf{1}\cdot CH_2Cl_2$ (0.13 g, 0.26 mmol) in dichloromethane (5 mL). The mixture was stirred overnight upon which a light green solid was formed. The precipitate was filtered off, washed with dichloromethane (2 × 5 mL) and diethyl ether (2 × 5 mL), and dried under vacuum, yielding 0.085 g of **7** (68%). Elemental analysis calcd (%) for $C_{22}H_{24}ClN_5O_2V$ (476.85): C 55.41, H 5.07, N 14.68, V 10.68; found C 55.15, H 5.22, N 14.52, V 10.59; $\mu_{eff} = 1.72\ \mu_B$ at 298 K.

[VOCl(Hcapca)]$\cdot 0.5\,CH_2Cl_2$ ($\mathbf{8}\cdot 0.5\,CH_2Cl_2$): Solid H_2capcah (0.30 g, 0.9 mmol) was added to a stirred solution of $[VOCl_2(thf)_2]$ (0.27 g, 0.9 mmol) in methanol (4 mL) at room temperature (20 °C). An immediate color change from blue to olive green concurrent with the precipitation of a green solid was observed. Addition of triethylamine (0.09 g, 0.9 mmol) to the mixture resulted in immediate color change from green to brown accompanied by dissolution of the green precipitate and the formation of a brown solid. The mixture was stirred for 3 h and filtered, and the light brown compound washed with dichloromethane (2 × 10 mL) and diethyl ether (2 × 10 mL), and dried in vacuo to afford 0.24 g of $\mathbf{8}\cdot 0.5\,CH_2Cl_2$ (60%). Elemental analysis calcd (%) for $C_{18.5}H_{16}Cl_{1.5}N_4O_2V$ (448.19): C 49.58, H 3.60, N 12.50, V 11.36; found C 49.50, H 3.87, N 12.60, V 11.29. Crystals of $\mathbf{8}\cdot CHCl_3$ suitable for X-ray structure analysis were obtained by vapor diffusion of diethyl ether into a saturated solution of $\mathbf{8}\cdot 0.5\,CH_2Cl_2$ in chloroform at 4 °C. $\mu_{eff} = 1.80\ \mu_B$ at 298 K.

[VO(NCS)(Hcapcah)] (9): Compound **9** was synthesized in 80% yield in an analogous fashion to complex **2**, except that $\mathbf{8}\cdot 0.5\,CH_2Cl_2$, was used instead

of $\mathbf{1}\cdot CH_2Cl_2$. Elemental analysis calcd (%) for $C_{19}H_{15}N_5O_2SV$ (428.36): C 53.27, H 3.53, N 16.35, V 11.89; found C 52.36, H 3.45, N 16.29, V 11.81. Crystals of $\mathbf{9}\cdot 2CH_3CN$ suitable for X-ray structure analysis were obtained by vapor diffusion of diethyl ether into a saturated solution of **9** in acetonitrile at 4 °C. $\mu_{eff} = 1.68\ \mu_B$ at 298 K.

[VO(N$_3$)(Hcapcah)]·2CH$_3$OH (10·2CH$_3$OH): Compound **10** was prepared in 55% yield in an analogous fashion to **3**, except that $\mathbf{8}\cdot 0.5\,CH_2Cl_2$ was used instead of $\mathbf{1}\cdot CH_2Cl_2$. Elemental analysis calcd (%) for $C_{20}H_{23}N_7O_4V$ (476.39): C 50.42, H 4.06, N 20.58, V 10.69; found C 50.25, H 4.75, N 20.52, V 10.72. Crystals of $\mathbf{10}\cdot CH_3CN$ suitable for X-ray structure analysis were obtained by vapor diffusion of diethyl ether into a saturated solution of $\mathbf{10}\cdot 2CH_3OH$ in acetonitrile at 4 °C. $\mu_{eff} = 1.66\ \mu_B$ at 298 K.

[VO(Hcapcah)(imidazole)]Cl (11) and [VO(Hcapcah)(imidazole)]BF$_4$ (12): Solid imidazole (0.027 g, 4 mmol) was added in one portion to a stirred suspension of $\mathbf{8}\cdot 0.5\,CH_2Cl_2$ (0.089 g, 0.19mmol) in methanol (4 mL). Upon addition of the imidazole, the solution cleared and turned from light to dark brown. After being stirred overnight, the reaction mixture was evaporated to dryness, and the solid was triturated with diethyl ether ($2\times$ 5 mL) and dried under vacuum to get 0.076 g of **11** (85%). Elemental analysis calcd (%) for $C_{21}H_{19}ClN_6O_2V$ (473.81): C 53.23, H 4.04, Cl 7.48, N 17.74, V 10.75; found C 53.15, H 4.30, Cl 7.31, N 17.90, V 10.70; $\mu_{eff} = 1.64\ \mu_B$ at 298 K. An equivalent of $AgBF_4$ was added in one portion to a stirred saturated solution of **11** in methanol. Upon addition of the silver salt a white precipitate (AgCl) was formed. Stirring was continued for ~3 h, and then the reaction mixture was filtered off. Vapour diffusion of diethyl ether into the filtrate at 4 °C resulted in the formation of crystals of [VO(Hcapcah)(imidazole)]BF_4 (**12**) suitable for X-ray structure analysis.

X-ray crystallography: Diffraction measurements for $\mathbf{9}\cdot 2CH_3CN$, $\mathbf{10}\cdot CH_3CN$ and **12** were performed on a Crystal Logic Dual Goniometer diffractometer with graphite monochromated $Mo_{K\alpha}$ radiation, while for $\mathbf{8}\cdot CHCl_3$ data collection was performed on a $P2_1$ Nicolet diffractometer upgraded by Crystal Logic with graphite monochromated $Cu_{K\alpha}$ radiation. Unit-cell dimensions (Table 6) were determined and refined by using the angular settings of 25 automatically centered reflections. Intensity data were recorded using a $\theta-2\theta$ scan. Three standard reflections monitored every 97 reflections showed less than 3% variation and no decay. Lorentz, polarization, and psi-scan absorption corrections were applied by using Crystal Logic software. The structures were solved by direct methods by using SHELXS-86[57] and refined by full-matrix least-squares techniques on F^2 with SHELXL-93.[58]

Further crystallographic details for $\mathbf{8}\cdot CHCl_3$: $2\theta_{max} = 121°$, scan speed 3.0° min^{-1}, scan range $3.0 + \alpha_1\alpha_2$ separation, reflections collected/unique/used = 3447/3276 [$R_{int} = 0.0290$]/3276, 335 parameters refined, $R1/wR2$ (for all data) = 0.0675/0.1523, $[\Delta\rho]_{min}/[\Delta\rho]_{max} = 0.436/-0.440$ e Å^{-3}, $[\Delta/\sigma] = 0.012$. All hydrogen atoms were located by difference maps and were refined isotropically, while all non-H atoms were refined anisotropically.

Further crystallographic details for $\mathbf{9}\cdot 2CH_3CN$: $2\theta_{max} = 49°$, scan speed 4.5° min^{-1}, scan range $2.3 + \alpha_1\alpha_2$ separation, reflections collected/unique/used = 4412/4114 [$R_{int} = 0.0244$]/4114, 396 parameters refined, $R1/wR2$ (for all data) = 0.0718/0.1457, $[\Delta\rho]_{min}/[\Delta\rho]_{max} = 0.343/-0.491$ e Å^{-3}, $[\Delta/\sigma] = 0.034$. All hydrogen atoms (except those on C21 which were introduced at calculated positions as riding on bonded atom) were located by difference maps and were refined isotropically, while all non-H atoms were refined anisotropically.

Further crystallographic details for $\mathbf{10}\cdot CH_3CN$: $2\theta_{max} = 50°$, scan speed 3.0° min^{-1}, scan range $2.3 + \alpha_1\alpha_2$ separation, reflections collected/unique/used = 3945/3722 [$R_{int} = 0.0147$]/3722, 342 parameters refined, $R1/wR2$ (for all data) = 0.0586/0.1243, $[\Delta\rho]_{min}/[\Delta\rho]_{max} = 0.513/-0.475$ e Å^{-3}, $[\Delta/\sigma] = 0.208$. All hydrogen atoms (except those of C20 which were introduced at calculated positions as riding on bonded atom) were located by difference maps and were refined isotropically, while all non-H atoms were refined anisotropically.

Further crystallographic details for **12**: $2\theta_{max} = 50°$, scan speed 3.0° min^{-1}, scan range $2.2 + \alpha_1\alpha_2$ separation, reflections collected/unique/used = 4131/3985 [$R_{int} = 0.0126$]/3985, 392 parameters refined, $R1/wR2$ (for all data) = 0.0695/0.1473, $[\Delta\rho]_{min}/[\Delta\rho]_{max} = 0.565/-0.349$ e Å^{-3}, $[\Delta/\sigma] = 0.006$. All hydrogen atoms were located by difference maps and were refined isotropically. All non-H atoms were refined anisotropically.

Crystallographic data (excluding structure factors) for the structures reported in this paper have been deposited with the Cambridge Crystallographic Data Centre as supplementary publication no. CCDC-152700 ($\mathbf{8}\cdot CHCl_3$), CCDC-152701 ($\mathbf{9}\cdot 2CH_3CN$), CCDC-152702 ($\mathbf{10}\cdot CH_3CN$), and CCDC-152703 (**12**). Copies of the data can be obtained free of charge on application to CCDC, 12 Union Road, Cambridge CB2 1EZ, UK (fax: (+44) 1223-336-033; e-mail: deposit@ccdc.cam.ac.uk).

Physical measurements: IR spectra were recorded on a Perkin–Elmer Spectrum G-X FT-IR system in KBr pellets. Electronic absorption spectra were measured as solutions in septum-sealed quartz cuvettes on a Jasco V570 UV/Vis/NIR spectrophotometer. Magnetic moments were measured at room temperature by the Faraday method, with mercuric tetrathiocyanatocobaltate(II) as the susceptibility standard on a Cahn-Vetron RM-2 balance. The ^1H and ^{13}C NMR spectra of the ligand H_2capcah were recorded on a Bruker AMX400 spectrometer, at 298 K, while its electron impact mass spectral data were obtained with a Kratos MS25RF A spesctrometer. The melting point of H_2capcah was determined (uncorrected) with a Buchi melting point apparatus.

EPR studies: Continuous-wave EPR spectra were recorded at liquid helium temperatures with a Bruker ER200 X-band spectrometer equipped with an Oxford Instruments cryostat. The microwave frequency and the magnetic field were measured with a microwave-frequency counter HP 5350B and a Bruker ER035M NMR gaussmeter, respectively. The temperature was monitored with an Oxford ITC5 temperature controller equipped with a calibrated AuFe (0.007 Chr) thermocouple. For the EPR measurements the oxovanadium(IV) compounds were dissolved in the appropriate solvent at room temperature (~20 °C) with subsequent freezing in liquid nitrogen. The program SIMFONIA version 2.1 by Bruker was used for numerical simulation of the EPR spectra for an $S = 1/2$ electron spin coupled to the $I = 7/2$ nuclear spin from the ^{51}V nucleus. No resolvable improvement of the

Table 6. Summary of crystallographic data for compounds **8**–**10** and **12**.

	$\mathbf{8}\cdot CHCl_3$	$\mathbf{9}\cdot 2CH_3CN$	$\mathbf{10}\cdot CH_3CN$	**12**
formula	$C_{19}H_{16}Cl_4N_4O_2V$	$C_{23}H_{21}N_7O_2SV$	$C_{20}H_{18}N_8O_2V$	$C_{21}H_{19}BF_4N_6O_2V$
M_r	525.10	510.47	453.36	525.17
a [Å]	9.312(3)	8.596(6)	18.021(9)	13.85(1)
b [Å]	10.222(3)	19.01(1)	11.692(7)	10.791(8)
c [Å]	12.354(4)	15.16(1)	10.187(6)	16.29(1)
α [°]	79.03(1)			
β [°]	70.70(1)	93.02(2)	99.50(2)	111.57(3)
γ [°]	81.69(1)			
V [Å^3]	1085.3(6)	2474(3)	2117(2)	2265(3)
Z	2	4	4	4
ρ_{calcd} [Mg m^{-3}]	1.607	1.371	1.423	1.540
space group	$P\bar{1}$	$P2_1/c$	$P2_1/a$	$P2_1/n$
T [K]	298	298	298	298
radiation/λ [Å]	$Cu_{K\alpha}$/1.5418	$Mo_{K\alpha}$/0.710730	$Mo_{K\alpha}$/0.710730	$Mo_{K\alpha}$/0.710730
μ [mm^{-1}]	8.565	0.519	0.503	0.503
octants collected	$\pm h, \pm k, -l$	$h, -k, \pm l$	$\pm h,k,l$	$\pm h,k,l$
GOF on F^2	1.057	1.092	1.089	1.019
$R1$	0.0518[a]	0.0513[b]	0.0455[c]	0.0508[d]
$wR2$	0.1347[a]	0.1333[b]	0.1168[c]	0.1324[d]

[a] For 2672 reflections with $I > 2\sigma(I)$. [b] For 3119 reflections with $I > 2\sigma(I)$. [c] For 3047 reflections with $I > 2\sigma(I)$. [d] For 3045 reflections with $I > 2\sigma(I)$.

0947-6539/01/0712-2708 $ 17.50+.50/0 *Chem. Eur. J.* **2001**, *7*, No. 12

simulations could be achieved by considering noncollinear g and hyperfine tensor A; thus these two tensors are considered to be collinear.

Computational details: The electronic structure and geometries of the actual complexes and the models studied were computed within the density functional theory by using gradient corrected functionals at the Becke3LYP computational level.[59, 60] The effective core potential (ECP) approximation of Hay and Wadt was used.[61–63] For the V atom, the electrons described by the ECP were those of 1s, 2s, and 2p shells. The basis set used was of valence double-quality.[64] Full geometry optimizations were carried out without no symmetry constraint. For the model molecules a frequency calculation after each geometry optimization ensured that the calculated structure was a real minimum in the potential energy surface of the molecule. All of the calculations were performed by using the Gaussian-98 package.[65]

Acknowledgements

We gratefully acknowledge support of this research by the Greek General Secretariat of Research and Technology (Grant no. 1807/95), the General Secretariat of Athletics (OPAP), and A. Athanasiou; we thank F. Masala for typing the manuscript.

[1] S. W. Taylor, B. Kammerer, E. Bayer, *Chem. Rev.* **1997**, *97*, 333.
[2] R. E. Berry, E. M. Armstrong, R. L. Beddoes, D. Collison, S. N. Ertok, M. Helliwell, C. D. Garner, *Angew. Chem.* **1999**, *111*, 871; *Angew. Chem. Int. Ed.* **1999**, *38*, 795.
[3] T. Ishii, I. Nakai, C. Numako, K. Ohoshi, K. Otake, *Naturwissenschaften* **1993**, *80*, 268.
[4] a) I. Harvey, J. M. Arber, R. R. Eady, B. E. Smith, C. D. Garner, S. S. Hasnain, *Biochem. J.* **1990**, *266*, 929; b) J. Chen, J. Christiansen, R. C. Tittsworth, B. J. Hales, S. J. George, D. Coucouvanis, S. P. Cramer, *J. Am. Chem. Soc.* **1993**, *115*, 5509.
[5] S. Macedo-Ribeiro, W. Hemrika, R. Revirie, R. Wever, A. Messerschmidt, *J. Biol. Inorg. Chem.* **1999**, *4*, 209, and references therein.
[6] a) D. C. Crans, A. D. Keramidas, H. Hoover-Litty, O. P. Anderson, M. M. Miller, L. M. Lemoine, S. Pleasu-Williams, M. Vandenberg, A. J. Rossomando, L. J. Sweet, *J. Am. Chem. Soc.* **1997**, *119*, 5447; b) S. S. Amin, K. Cryer, B. Zhang, S. K. Dutta, S. S. Geaton, O. P. Anderson, S. M. Miller, B. A. Reul, S. M. Brichard, D. C. Crans, *Inorg. Chem.* **2000**, *39*, 406; c) K. H. Thompson, J. H. McNeill, C. Orving, *Chem. Rev.* **1999**, *99*, 2561; d) K. H. Thompson, C. Orving, *J. Chem. Soc. Dalton Trans.* **2000**, 2885.
[7] a) D. Rehder, *Met. Ions Biol. Syst.* **1995**, *31*, 1; b) D. Rehder, *Coord. Chem. Rev.* **1999**, *182*, 297.
[8] N. D. Chasteen, in *Biological Magnetic Resonance*, *Vol. 3* (Eds.: L. Berliner, J. Reuben), Plenum, New York, **1981**, pp. 53–119.
[9] a) J. J. Fitzgerald, N. D. Chasteen, *Biochemistry* **1974**, *13*, 4338. b) R. J. DeKoch, D. J. West, J. C. Cannon, N. D. Chasteen, *Biochemistry* **1974**, *13*, 4347.
[10] N. D. Chasteen, R. J. DeKoch, B. L. Rogers, M. W. J. Hanna, *J. Am. Chem. Soc.* **1973**, *95*, 1301.
[11] J. Nieves, L. Kim, D. Puett, L. Echegoyen, J. Benabe, M. Martinez-Maidonado, *Biochemistry* **1987**, *26*, 4523.
[12] E. De Boer, C. P. Keijers, A. A. K. Klaassen, E. J. Reijerse, D. Collison, C. D. Garner, R. Wever, *FEBS Lett.* **1988**, *235*, 93.
[13] P. A. Tipton, J. McCracken, J. B. Cornelius, J. Peisach, *Biochemistry* **1989**, *28*, 5720.
[14] S. S. Eaton, J. Dubach, K. M. More, G. R. Eaton, G. Thurman, D. B. Ambuse, *J. Biol.* Chem. **1989**, *264*, 4776.
[15] R. P. Ferrari, *Inorg. Chim. Acta* **1990**, *176*, 83.
[16] P. M. Hanna, N. D. Chasteen, G. A. Rottman, P. Aisen, *Biochemistry* **1991**, *30*, 9210.
[17] C. Zhang, G. D. Markham, R. LoBrutto, *Biochemistry* **1993**, *32*, 9866.
[18] A. L. P. Houseman, L. Morgan, R. LoBrutto, W. P. Frasch, *Biochemistry* **1994**, *33*, 4910.
[19] S. A. Dikanov, A. M. Tyryshkin, J. Hüttermann, R. Bogumil, H. Witzel, *J. Am. Chem. Soc.* **1995**, *117*, 4976.
[20] D. Mustafi, Y. Nakagawa, *Biochemistry* **1996**, *35*, 14703.
[21] J. Petersen, T. R. Hawkes, D. J. Lowe, *J. Am. Chem. Soc.* **1998**, *120*, 10978.
[22] K. Fukui, H. Ohya-Nishiguchi, H. Kamada, *Inorg. Chem.* **1998**, *37*, 2326.
[23] R. LoBrutto, B. J. Hamstra, G. J. Colpas, V. L. Pecoraro, W. D. Frasch, *J. Am. Chem. Soc.* **1998**, *120*, 4410.
[24] a) C. V. Grant, J. A. Ball, B. J. Hamstra, V. L. Pecoraro, R. D. Britt, *J. Phys. Chem. B* **1998**, *102*, 8145; C. V. Grant, W. Cope, J. A. Ball, G. G. Maresch, B. J. Gaffney, W. Fink, R. D. Britt, *J. Phys. Chem. B* **1999**, *103*, 10627; b) C. V. Grant, K. M. Geiser-Bush, C. Cornman, R. D. Britt, *Inorg. Chem.* **1999**, *38*, 6285.
[25] C. J. Ballhausen, H. B. Gray, *Inorg. Chem.* **1962**, *1*, 111.
[26] A. J. Tasiopoulos, A. N. Troganis, A. Evangelou, C. P. Raptopoulou, A. Terzis, Y. Deligiannakis, T. A. Kabanos, *Chem. Eur. J.* **1999**, *5*, 910.
[27] L. J. Boucher, E. C. Tynan, T. F. Yen, in *ESR of Metal Complexes*, Plenum, New York, **1969**, pp. 110–13.
[28] H. Sakurai, J. Hirata, H. Michibata, *Biochem. Biophys. Res. Commun.* **1987**, *149*, 411.
[29] E. J. Tolis, K. D. Soulti, C. P. Raptopoulou, A. Terzis, Y. Deligiannakis, T. A. Kabanos, *Chem. Commun.* **2000**, 601.
[30] a) L. J. Calviou, J. M. Arber, D. Collison, C. D. Garner and W. Clegg, *J. Chem. Soc. Chem. Commun.* **1992**, 654; b) M. Mohan, M. R. Bond, T. Otieno and C. J. Carrano, *Inorg. Chem.* **1995**, *34*, 1233. In these two papers are reported the *only* two structurally characterized $V^{IV}O^{2+}$ compounds that contain the unit *trans*-{V(=O)Cl} and have N_4 equatorial-donor-atom sets, namely: $[VOCl(1\text{-vinylimidazole})_4]^+$ and $[VOCl(pyrazole)_4]^+$ with A_z values of 162 and $176 \times 10^{-4}\,cm^{-1}$, respectively. The A_z value for compound $[VOCl(pyrazole)_4]^+$ is characteristic of an equatorial donor set dominated by oxygens, most likely indicating decomposition of the complex in the solvent system (water/glycerine) used. The A_z value for $[VOCl(1\text{-vinylimidazole})_4]^+$ is in the expected range for an N_4 equatorial-donor-atom system.
[31] a) C. J. Carrano, C. N. Nunn, R. Quan, J. A. Bonadies, V. Pecoraro, *Inorg. Chem.* **1990**, *29*, 944; b) T. A. Kabanos, A. D. Keramidas, A. Terzis, *J. Chem. Soc. Chem. Commun.* **1990**, 1664; c) G. R. Hanson, T. A. Kabanos, A. D. Keramidas, D. Mentzafos, A. Terzis, *Inorg. Chem.* **1992**, *31*, 2587.
[32] a) T. A. Kabanos, A. D. Keramidas, A. B. Papaionannou, A. Terzis, *J. Chem. Soc. Chem. Commun.* **1993**, 643; b) A. S. Borovik, T. W. Dewey, K. N. Raymond, *Inorg. Chem.* **1993**, *32*, 413; c) A. D. Keramidas, A. B. Papaionnou, A. Vlahos, T. A. Kabanos, G. Bonas, A. Makriyannis, C. P. Raptopoulou, A. Terzis, *Inorg. Chem.* **1996**, *35*, 357 and references therein.
[33] a) H. Kelm, H. J. Krüger, *Inorg. Chem.* **1996**, *35*, 3533; b) T. A. Kabanos, A. D. Keramidas, A. Papaioannou, A. Terzis, *Inorg. Chem.* **1994**, *33*, 845.
[34] a) A. Neves, W. Walz, K. Wieghardt, B. Nuber, J. Weiss, *Inorg. Chem.* **1988**, *27*, 2484; b) S. G. Brand, N. Edelstein, C. J. Hawkins, G. Shalimoff, M. R. Snow, E. R. T. Tiekink, *Inorg. Chem.* **1990**, *29*, 434; c) M. A. A. F. de C. T. T. Carrondo, M. T. L. S. Duarte, J. A. L. Silva, J. J. R. Frausto da Silva, *Polyhedron* **1991**, *10*, 73; d) P. Basu, S. Pal, A. J. Chakravorty, *J. Chem. Soc. Dalton Trans.* **1991**, 3217; e) J. Chakravarty, S. Dutta, S. K. Chandra, P. Basu, A. Chakravorty, *Inorg. Chem.* **1993**, *32*, 4249; f) I. Cavaco, J. C. Pessoa, D. Costa, M. T. Duarte, R. D. Gillard, P. Matias, *J. Chem. Soc. Dalton Trans.* **1994**, 149; g) B. J. Hamstra, A. L. P. Houseman, G. J. Colpas, J. W. Kampt, R. Lobrutto, W. D. Frasch, V. L. Pecoraro, *Inorg. Chem.* **1997**, *36*, 4866; h) K. Kanamori, I. Kazuhito, K. I. Okamoto, *Acta Crystallogr. Sect. C* **1997**, *53*, 672; i) K. Kanamori, K. Miyazaki, K. I. Okamoto, *Acta Crystallogr. Sect. C* **1997**, *53*, 673.
[35] The V–Cl and V=O bond lengths in mononuclear octahedral compounds that contain the unit *cis*-{$V^{IV}OCl$} range from 2.295 to 2.400 and from 1.579 to 1.624 Å, respectively; see references [26, 33] and a) G. R. Willey, M. T. Lakin, N. W. Alcock, *J. Chem. Soc. Chem. Commun.* **1991**, 1414; b) J. Zah-Letho, E. Samuel, Y. Dromzee, Y. Jeannin, *Inorg. Chim. Acta* **1987**, *126*, 35; c) W. Priebsch, D. Rehder, *Inorg. Chem.* **1990**, *29*, 3013;
[36] a) C. R. Cornman, J. Kampf, M. S. Lah, V. L. Pecoraro, *Inorg. Chem.* **1992**, *31*, 2035; b) T. S. Smith, C. A. Root, J. W. Kampf, P. G. Rasmussen, V. L. Pecoraro, *J. Am. Chem. Soc.* **2000**, *122*, 767.
[37] The d–d transition does not appear in **3** and **6**·CH_3NO_2, owing to very low solubility in CH_3OH of these compounds. Methanol is the

solvent in which these two oxo-vanadium(IV) compounds have their maximum solubility.
[38] D. J. Barnes, R. L. Chapman, F. S. Stephens, R. S. Vagg, *Inorg. Chim. Acta* **1981**, *51*, 155.
[39] R. J. H. Clark, C. S. Williams, *Inorg. Chem.* **1965**, *4*, 350.
[40] K. Nakamoto, *Infrared and Raman Spectra of Inorganic and Coordination Compounds*, 4th ed., Wiley, New York, **1986**.
[41] Z. Dori, R. F. Ziolo, *Chem. Rev.* **1973**, *73*, 247.
[42] G. B. Deacon, R. J. Phillips, *Coord. Chem. Rev.* **1980**, *33*, 227.
[43] S. A. Dikanov, Y. D. Tsvetkov, *Electron Spin Echo Envelope Modulation (ESEEM) Spectroscopy*, CRC, Boca Raton, FL, **1992**.
[44] Y. Deligiannakis, A. W. Rutherford, *J. Am. Chem. Soc.* **1997**, *119*, 4471.
[45] A. Jezierski, J. B. Raynor, *J. Chem. Soc. Dalton Trans.* **1981**, 1.
[46] a) S. G. Brand, MSc Thesis, University of Queensland, **1987**; b) D. Sanna, G. Micera, L. S. Erre, M. G. Molinu, E. Garriba, *J. Chem. Research (S)* **1996**, 40.
[47] A. J. Tasiopoulos, Y. G. Deligiannakis, J. D. Woollins, A. M. Z. Slawin, T. A. Kabanos, *Chem. Commun.* **1998**, 569.
[48] T. B. Wen, J. C. Shi, X. Huang, Z. N. Chen, Q. T. Liu, B. S. Kang, *Polyhedron* **1998**, *17*, 331.
[49] J. C. Dutton, G. D. Fallon, K. S. Murray, *Inorg. Chem.* **1988**, *27*, 34.
[50] J. K. Money, K. Folting, J. C. Huffman, D. Collison, J. Tempertey, F. E. Mabbs, Christou, *Inorg. Chem*. **1986**, *25*, 4583.
[51] In order to work out the calculated A_z values of **1**–**9** and **11**, we used the following A_z contributions: $N_{pyr} = 40.7$, $-CON^{-}- = 35$, $-C{=}N- = 44.1$, $Cl^- = 44.2$, $-HN_{amine}- = 40.1$, $-NCS^- = 43.2$ (From reference: C. M. Mulks, B. Kriste, H. van Willigen, *J. Am. Chem. Soc.* **1982**, *104*, 5906), $N_{imidazole} = 40.0$. All in units of $10^{-4}\,cm^{-1}$. The calculated A_z value of compound $\mathbf{10}\cdot 2CH_3OH$ was not reported because the A_z contribution of N_3^- has not been reported in the literature.
[52] B. R. McGarvey, *Trans. Met. Chem.* **1966**, *3*, 89.
[53] D. Kivelson, S. K. Lee, *J. Chem. Phys.* **1964**, *41*, 1896.
[54] A. Davinson, N. Edelstein, R. H. Holm, A. H. Maki, *J. Am. Chem. Soc.* **1964**, *86*, 2799.
[55] J. Selbin, *Coord. Chem. Rev.* **1966**, 293.
[56] R. G. Kern, *J. Inorg. Nucl. Chem.* **1962**, *24*, 1105.
[57] G. M. Sheldrick, *SHELXS-86: Structure Solving Program*, University of Gottingen (Germany), **1986**.
[58] G. M. Sheldrick, *SHELXS-97: Crustal Structure Refinement Program*, University of Gottingen (Germany), **1997**.
[59] D. Becke, *J. Chem. Phys* **1993**, *98*, 5648.
[60] Lee, W. Yang and R. G. Parr, *Phys. Rev. B* **1988**, *37*, 785.
[61] P. J. Hay and W. R. Wadt, *J. Chem. Phys.* **1985**, *82*, 270.
[62] W. R. Wadt and P. J. Hay, *J. Chem. Phys.* **1985**, *82*, 284.
[63] P. J. Hay and W. R. Wadt, *J. Chem. Phys.* **1985**, *82*, 299.
[64] T. H. Dunning Jr., P. J. Hay, in *Modern Theoretical Chemistry*, *Vol. 3* (Ed.: H. F. Schaefer, III) Plenum, New York, **1976**, p. 1.
[65] M. J. Frisch, G. W. Trucks, H. B. Schlegel, G. E. Scuseria, M. A. Robb, J. R. Cheeseman, V. G. Zakrzewski, J. A. Montgomery, Jr., R. E. Stratmann, J. C. Burant, S. Dapprich, J. M. Millam, A. D. Daniels, K. N. Kudin, M. C. Strain, O. Farkas, J. Tomasi, V. Barone, M. Cossi, R. Cammi, B. Mennucci, C. Pomelli, C. Adamo, S. Clifford, J. Ochterski, G. A. Petersson, P. Y. Ayala, Q. Cui, K. Morokuma, D. K. Malick, A. D. Rabuck, K. Raghavachari, J. B. Foresman, J. Cioslowski, J. V. Ortiz, B. B. Stefanov, G. Liu, A. Liashenko, P. Piskorz, I. Komaromi, R. Gomperts, R. L. Martin, D. J. Fox, T. Keith, M. A. Al-Laham, C. Y. Peng, A. Nanayakkara, C. Gonzalez, M. Challacombe, P. M. W. Gill, B. G. Johnson, W. Chen, M. W. Wong, J. L. Andres, M. Head-Gordon, E. S. Replogle, J. A. Pople, *Gaussian 98*, *Revision A.1*, Gaussian, Pittsburgh PA, **1998**.

Received: November 20, 2000 [F2885]

  0947-6539/01/0712-2710 $ 17.50+.50/0